

## Determination of the Adsorption Site by Low-Energy Electron Diffraction for Iodine on Silver (111)

F. Forstmann, W. Berndt, and P. Büttner

*Fritz-Haber-Institut der Max-Planck-Gesellschaft, Berlin-Dahlem, Germany*

(Received 27 November 1972)

Iodine adsorbing on a silver (111) surface forms a  $(\sqrt{3} \times \sqrt{3})30^\circ$  structure. The position of the adsorbed atoms within the unit cell of the surface layer has been determined by comparison of the measured curves of intensity versus energy of several low-energy electron diffraction spots with dynamical model calculations.

Recently, it has been shown by several authors<sup>1-5</sup> that the intensities of low-energy electron diffraction (LEED) from clean metal surfaces can be calculated in good agreement with experiment if multiple scattering theory is applied to "realistic" models. One can then extend the same method of computation to determine the sites of adsorbed atoms relative to the underlying substrate layer. This was successfully done for the first time by Andersson and Pendry<sup>6</sup> for sodium on nickel. In the present paper it is reported that the model calculations lead to a safe conclusion about the adsorbate position also in the case of an electronegative adsorbed species like iodine.

Iodine adsorbs on (111) silver forming a  $(\sqrt{3} \times \sqrt{3})30^\circ$  structure. This deposition is accompanied by an increase of the work function by 0.35 eV, which was measured by the retarding-potential method. The iodine can be easily desorbed again by heating to 200°C, which indicates a weak adsorption bond without surface reconstruction. The sticking probability is low. The iodine layer was formed by adsorption from the gas phase at room temperature with an iodine pressure of  $7 \times 10^{-8}$  Torr. An exposure to  $20 \times 10^{-6}$  Torr sec was necessary for the formation of the ordered iodine layer. The mass-spectrometer analysis of the residual gas shows that  $I_2$  disappears quickly after closing the leak valve. When heating the system, only I is found. This supports the assumption that iodine is dissociated when it is adsorbed.

These results lead to the model of an ordered iodine overlayer with 1 atom per unit cell of the adsorbate structure, i.e., 1 iodine atom per 3 silver atoms. This layer is relatively close packed because the distance between the adsorbed atoms (4.98 Å) is only 9% larger than the I-I distance in AgI. In the unit cell there are probable positions for the iodine atom (Fig. 1). Two of them are above hollows with threefold symmetry, "billiard-ball positions," the third is on top

of a silver atom. The saddle positions between two silver atoms are unlikely, because they have no axial symmetry. Positions 1 and 2 are different from each other with respect to the second silver layer: Below position 2 there is a silver atom, while there is none below position 1.

The proper site and the distance between the iodine layer and the silver surface can only be determined by an investigation of the LEED intensities. These were measured by a spot photometer and in case of the (00) beam in addition by a Faraday cup. Both methods agreed quantitatively. With the Faraday cup the photometer intensities could be calibrated. The incident beam was tilted by  $8^\circ$  from the (111) surface normal, the plane of incidence was  $(01\bar{1})$ , the tangential component of the incident beam pointed towards  $[\bar{2}11]$ . These conditions give twofold symmetry which was incorporated into the calculations.

The intensity calculations were carried out by use of a method suggested by Pendry.<sup>7</sup> The absorption is assumed to be strong in the energy range 20–130 eV. With an imaginary potential  $V_{0i} = -4$  eV one gets excellent agreement for the intensities from the clean silver surface.<sup>8</sup> With this high absorption, we used Pendry's renormal-

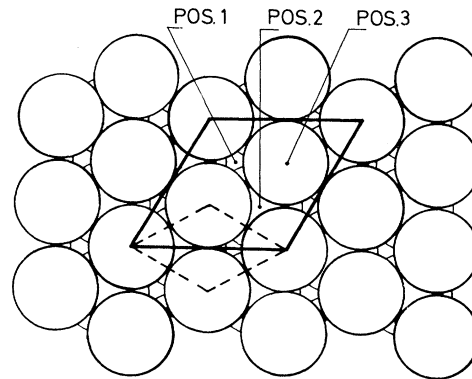


FIG. 1. Silver surface layer with the unit cell of the adsorbate structure. The considered adsorbate positions are indicated.

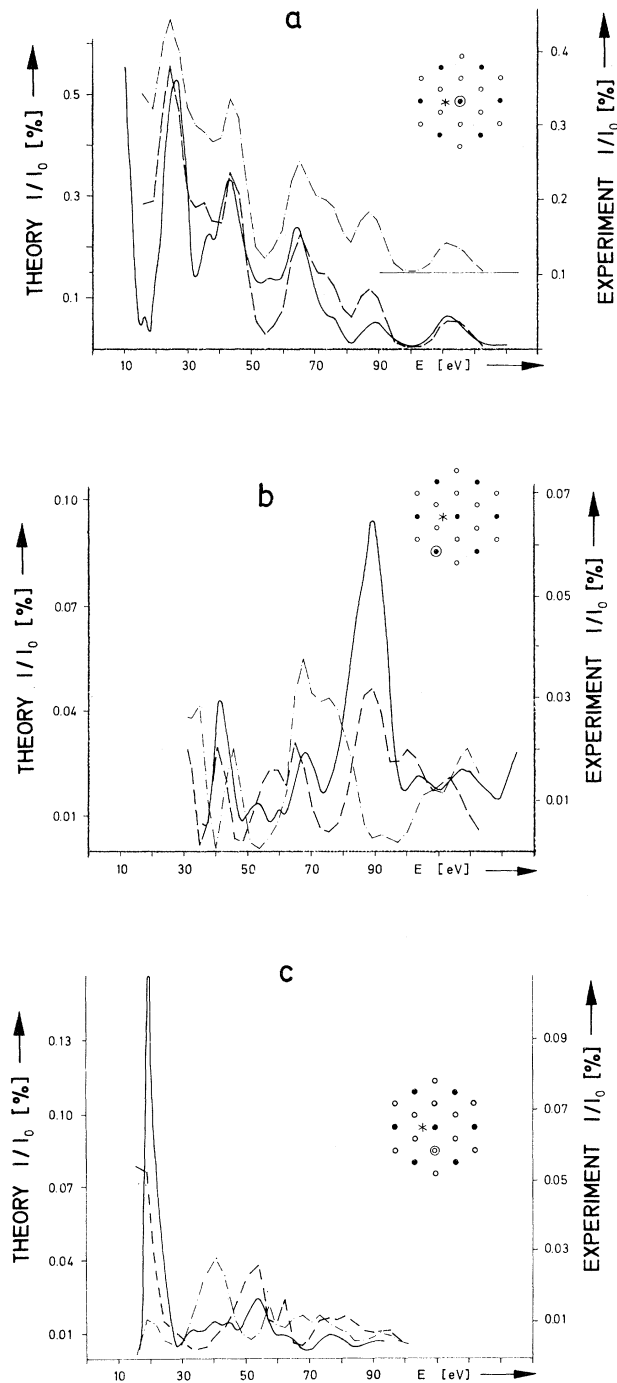


FIG. 2. (a)–(c) Intensity-versus-energy curves from a  $(\sqrt{3} \times \sqrt{3})30^\circ$  iodine structure on a silver (111) surface at an incidence angle of  $8^\circ$  from normal. The corresponding diffraction spot is encircled in the pattern. The asterisk indicates the electron gun position. Solid line, experiment; dashed line, theory for iodine in position 1; dot-dashed line, theory for iodine in position 2. The ratio between theoretical and experimental scales is 1.45.

ized forward-scattering perturbation scheme.<sup>9</sup> The scattering potentials for silver and iodine were determined from Hartree-Fock wave functions<sup>10</sup> for the Coulomb part with an exchange contribution according to Slater-Wilson-Wood.<sup>11</sup> For silver it turned out<sup>8</sup> that this energy-dependent exchange is an important improvement on the Slater exchange average. A full Hartree-Fock calculation as done by Pendry<sup>2</sup> seems to be unnecessary. For iodine we used the atomic potential, the ionic potential, and the average of the two corresponding sets of phase shifts.

The measured intensities are smaller than the calculated ones because of thermal movement of the scatterers. Lagally<sup>12</sup> has measured the temperature dependence of the (00) intensity for (111) silver and derived Debye-Waller factors. These can be approximated by  $f(E) = \exp[-(0.065E + 1.5) \times 10^{-3}T]$  ( $E$  = electron in eV). The calculated intensities were multiplied by this factor.

An inner potential was finally determined by adjusting the zeros of the energy scales. For clean silver it was found to be  $V_{0s} = -10.5$  eV, and for the covered surface  $V_0 = -11$  eV was chosen because of the small increase in work function. The inner potential and the imaginary part of the potential of the iodine layer was set equal to that of the underlying silver in order not to introduce additional parameters. It turned out that the calculated curves of intensity versus energy of the specularly reflected beam were nearly independent of any lateral displacement of the iodine layer. Therefore one could find the layer distance and the best set of phase shifts for the adsorbed iodine by aiming at agreement between the experimental and theoretical 00 intensities. The result of this trial and error scheme is shown in Fig. 2(a). Best agreement is achieved if the adsorbed iodine is a distance of  $2.25 \text{ \AA}$  from the silver surface layer. Its scattering properties are best described by the phase shifts of an iodine atom. This small distance rules out position 3 which from plausible radii needs a distance of at least  $2.7 \text{ \AA}$ . The intensities for nonspecular beams were checked for position 3 and did not agree with the measurements. Figures 2(b) and 2(c) show the intensity curves for two nonspecular beams. Here, calculations for iodine in positions 1 and 2 are compared with experiment. This gives a clear decision for position 1.

The result is that iodine adsorbs on silver in the position where it "saturates the broken dangling bonds," and not at that site where it has as many neighbors as possible. Its distance of  $2.25$

Å from the silver surface gives an interatomic I-Ag distance of 2.8 Å which is the same as in the AgI crystal. Within our scheme, this distance could be determined with 5% accuracy.

We thank Dr. Pendry for supplying the main parts of the program for the intensity calculations and Dr. Kambe for many helpful discussions. We acknowledge the financial support of this work by the Deutsche Forschungsgemeinschaft.

<sup>1</sup>G. Capart, *Surface Sci.* **26**, 429 (1971).

<sup>2</sup>J. B. Pendry, *J. Phys. C: Proc. Phys. Soc., London* **4**, 2514 (1971).

<sup>3</sup>D. W. Jepsen, P. M. Marcus, and F. Jona, *Phys. Rev. B* **5**, 3933 (1972).

<sup>4</sup>S. Y. Tong and T. N. Rhodin, *Phys. Rev. Lett.* **26**, 711 (1971).

<sup>5</sup>G. E. Laramore, C. B. Duke, A. Bagchi, and A. B. Kunz, *Phys. Rev. B* **4**, 2058 (1971).

<sup>6</sup>S. Andersson and J. B. Pendry, *J. Phys. C: Proc. Phys. Soc., London* **5**, L41 (1972).

<sup>7</sup>J. B. Pendry, *J. Phys. C: Proc. Phys. Soc., London* **4**, 2501 (1971).

<sup>8</sup>F. Forstmann and W. Berndt, to be published.

<sup>9</sup>J. B. Pendry, *J. Phys. C: Proc. Phys. Soc., London* **4**, 3095 (1971).

<sup>10</sup>For silver, see M. Synek and F. Schmitz, *Phys. Lett.* **27A**, 349 (1968); for iodine, see M. Synek and A. Damommio, *Phys. Lett.* **28A**, 344 (1968).

<sup>11</sup>J. C. Slater, T. M. Wilson, and J. H. Wood, *Phys. Rev.* **179**, 28 (1969).

<sup>12</sup>M. G. Lagally, *Z. Naturforsch.* **25a**, 1567 (1970).

## Optical Properties of Ferromagnetic $K_2CrCl_4$

P. Day, A. K. Gregson, and D. H. Leech

*University of Oxford, Inorganic Chemistry Laboratory, Oxford, England*

(Received 7 November 1972)

The optical absorption spectrum of the ferromagnetic insulator  $K_2CrCl_4$  has been measured from 8000 to 25 000  $cm^{-1}$  and for temperatures between 4.2 and 300°K.

Ferromagnetic materials having discrete optical absorption bands, and hence regions of relative transparency in the visible, are rather uncommon. Indeed, in all the insulating ferromagnetic transition-metal compounds examined hitherto, the entire visible region is covered by a succession of broad overlapping ligand-field<sup>1</sup> or charge-transfer<sup>2</sup> bands. We now report preliminary optical studies of the three-dimensional ferromagnet  $K_2CrCl_4$ , the visible absorption of which is almost entirely concentrated into two narrow spectral regions, sufficiently resolved from each other to permit quantitative measurements of the temperature variation of their oscillator strengths.

$K_2CrCl_4$  is a member of an extensive series of ternary halides formed by alkali metals and divalent 3d elements.<sup>3,4</sup> X-ray powder photographs<sup>3</sup> indicated a structure very similar to that of  $Cs_2CrCl_4$ , which has the  $K_2NiF_4$  structure. This conclusion is confirmed by a single-crystal x-ray study,<sup>5</sup> which demonstrated that the unit cell is in fact orthorhombic ( $a=7.13$ ,  $b=7.34$ ,  $c=14.97$  Å), though the deviation from the tetragonal cell of the parent  $K_2NiF_4$  structure is small. The magnetic susceptibility of a powder sample measured between 80–300°K has been extrapolat-

ed to give a Weiss constant of  $+67 \pm 1$ °K.<sup>3</sup> Further analysis<sup>3,6</sup> of the same data using high-temperature series-expansion techniques<sup>7,8</sup> applicable to a Heisenberg ferromagnet having a plane square lattice with  $S=2$  yielded an exchange integral of  $5.0 \pm 0.5$   $cm^{-1}$ . Magnetization measurements over the range 4.2–80°K<sup>9</sup> confirm that the compound becomes ferromagnetic below 65°K.

Crystals of  $K_2CrCl_4$  were grown from the melt in a Bridgman furnace. Because the plane of easy cleavage is perpendicular to the  $c$  axis, and thin crystals were needed for measurements of the two intense sharp visible transitions, good quality spectra were only obtained for light propagated along this axis (Fig. 1). Poorer-quality spectra recorded with the incident light perpendicular to  $c$  showed that while the axial and  $\sigma$  spectra were very similar, the  $\pi$  absorption was much weaker.<sup>10</sup> By comparison with other Cr(II) spectra,<sup>11</sup> we assign the three broad bands between 8000 and 14 000  $cm^{-1}$  to the low-symmetry components of  ${}^5D$ . If, in common with all other Cr(II) salts having strongly Jahn-Teller distorted ground states, we assume that the Cr site in  $K_2CrCl_4$  is tetragonally elongated, the three bands are assigned to transitions from  ${}^5B_{1g}({}^5E_g)$  to  ${}^5A_{1g}({}^5E_g)$  and  $({}^5B_{1g} + {}^5E_g)({}^5T_{2g})$ .